Traceable Biogenic Nanovectors

DOI: 10.1002/anie.201410223

# Transformation of Cell-Derived Microparticles into Quantum-Dot-Labeled Nanovectors for Antitumor siRNA Delivery**

*Gang Chen, Jun-Yi Zhu, Zhi-Ling Zhang, Wei Zhang, Jian-Gang Ren, Min Wu, Zheng-Yuan Hong, Cheng Lv, Dai-Wen Pang,* and Yi-Fang Zhao**

***Abstract:*** *Cell-derived microparticles (MPs) have been recently recognized as critical intercellular information conveyors. However, further understanding of their biological behavior and potential application has been hampered by the limitations of current labeling techniques. Herein, a universal donor-cell-assisted membrane biotinylation strategy was proposed for labeling MPs by skillfully utilizing the natural membrane phospholipid exchange of their donor cells. This innovative strategy conveniently led to specific, efficient, reproducible, and biocompatible quantum dot (QD) labeling of MPs, thereby reliably conferring valuable traceability on MPs. By further loading with small interference RNA, QD-labeled MPs that had inherent cell-targeting and biomolecule-conveying ability were successfully employed for combined bioimaging and tumor-targeted therapy. This study provides the first reliable and biofriendly strategy for transforming biogenic MPs into functionalized nanovectors.*

Microparticles (MPs), also known as microvesicles or shedding vesicles, are a fascinating population of cell-derived membrane vesicles. They are nanosized (100 nm to 1000 nm) spherical structures formed by direct budding of the plasma membrane.[1] MPs are usually considered as miniature versions of cells since they can inherit comparable membrane lipids, surface antigens, cytoplasmic proteins, and nucleic acids from their donor cells. Recently, MPs have been recognized as novel and critical mediators for intercellular communication.[2] By conveying bioactive molecules from the donor cells to the recipient target cells, either locally or at a distance through circulation, MPs are able to function in a broad range of physiological processes, such as regulation of vascular homeostasis.[2] Meanwhile, a considerable increase in circulating MPs is also closely linked to various pathological events including angiogenesis, inflammation, atherosclerosis, thrombosis, and malignancy.[2,3] Moreover, recent studies have indicated that MPs, which possess natural biomolecule-transporting capacity, may hold great potential as novel delivery vehicles for theranostic purpose.[4–7] However, deficiencies in the knowledge of MPs' biological behavior and lack of good strategies for labeling and visualizing these nanosized particles, have hampered the identification of MPs and meanwhile posed great challenges for their potential applications.

Current approaches for optical visualization of MPs mainly rely on traditional fluorescent dyes, including carboxyfluorescein diacetate succinimidyl ester (CFSE), PKH26, and Calcein AM.[8] However, it has to be considered that MPs' biological behavior and their interplay with the recipient cells usually are complicated processes at the subcellular level. This is why long-term tracing and specific labeling techniques are required to investigate the biological behavior of MPs and meanwhile to discriminate them from the intrinsic structures of recipient cells, and the drawbacks of conventional organic fluorescent dyes, such as photobleaching, weak intensity, biodegradation, cytotoxicity, and nonspecific staining,[9] have largely restricted their application in labeling MPs. Thanks to the rapid progress in nanomaterial preparation, several pioneering works have been recently performed for coupling MPs with inorganic nanoparticles,[6,7] which can provide prominent advantages for the imaging of MPs. Nevertheless, there are still some key issues to be addressed to achieve a better combination of biogenic MPs and advanced nanoparticles. Firstly, the previously reported labeling of biogenic MPs, whether with fluorescent dyes or functional nanoparticles, was mostly realized by the "indirect encapsulation" strategy, namely, pre-incubation of the donor cells with different tags (dyes or nanoparticles) and then collection of the secreted MPs assumed to carry the tags. Such a strategy may easily give low efficiency and result in uneven outcomes, because it is highly dependent on the tag internalization by the donor cells and the enclosure of internalized tags into the secreted MPs, both of which are in fact nonselective and uncontrollable processes. Meanwhile, the metabolism process and intracellular environment of the donor cells are also under suspicion for causing harmfulness to the stability of internalized tags. Thus, the obtained MPs may actually contain a large subpopulation without any tags encapsulated and great variances may also exist among the

[*] Dr. G. Chen, Prof. Z. L. Zhang, M. Wu, Z. Y. Hong, C. Lv, Prof. D. W. Pang
Key Laboratory of Analytical Chemistry for Biology and Medicine (Ministry of Education), College of Chemistry and Molecular Sciences, and the Institute for Advanced Studies, Wuhan University
299 Bayi Road, Wuhan 430072 (China)
E-mail: dwpang@whu.edu.cn
Dr. G. Chen, J. Y. Zhu, Dr. W. Zhang, J. G. Ren, Prof. Y. F. Zhao
Key Laboratory of Oral Biomedicine (Ministry of Education) and Department of Oral and Maxillofacial Surgery, School and Hospital of Stomatology, Wuhan University
237 Luoyu Road, Wuhan 430079 (China)
E-mail: yifang@whu.edu.cn

[**] This work was supported by the National Basic Research Program of China (973 Program, 2011CB933600), the National Natural Science Foundation of China (81300895, 81170977 and 81371159), the Doctoral Program Foundation of Higher Education of China (20130141120089 and 20130141130006), and the China Postdoctoral Science Foundation (2013M540607).

Supporting information for this article is available on the WWW under http://dx.doi.org/10.1002/anie.201410223.

 © 2015 Wiley-VCH Verlag GmbH & Co. KGaA, Weinheim 

labeled MPs in terms of tag-carrying amount. Moreover, since MP generation is a tightly regulated and stimuli-sensitive process,[10] pre-incubation of their donor cells with different labeling materials, which are usually non-self components, may affect the MP formation process as well as the natural properties of MPs, thus posing obstacles to investigating their original behavior and functions. Considering the limitations of currently existing labeling approaches, it is highly desirable to develop a reliable and biofriendly strategy for more efficient and biocompatible labeling of biogenic MPs.

Previously, we have developed a number of reliable strategies for labeling nanosized organisms with fluorescent nanoparticles, and successfully revealed the infection mechanisms of multiple viruses.[11,12] More notably, based on the feature that viruses hijack their host cellular machineries for self-reproduction, we have established a universal host-cell-assisted methodology for surface labeling of enveloped viruses, which shows fascinating advantages such as convenient procedure, high efficiency, favorable biocompatibility, and good versatility.[13] Herein, by taking great advantage of the characteristic that MPs are formed by direct budding of the plasma membrane and meanwhile skillfully utilizing the natural biological process that phospholipids within the cell membrane are constantly and dynamically exchanged with the lipids from extracellular environment, we innovatively proposed a biofriendly and reliable donor-cell-assisted membrane biotinylation strategy for labeling cell-derived MPs. As shown in Scheme 1, the first step of our strategy is to obtain donor cells with a biotinylated membrane by culturing them in modified medium containing biotin-functionalized phosphatidylethanolamine (DSPE-PEG-biotin). The MPs, formed by direct budding from the plasma membrane of donor cells, will inherit the biotinylated membrane. Then, the biotinylated MPs can be directly labeled with streptavidin-conjugated quantum dots (SA-QDs) by utilizing the high affinity between biotin and streptavidin.

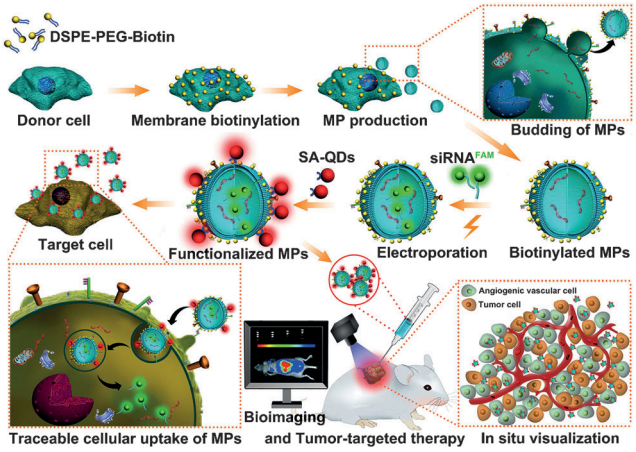


***Scheme 1.*** QD labeling of cell-derived MPs through a reliable and biofriendly donor-cell-assisted membrane biotinylation strategy, and its potential application in combined bioimaging and tumor-targeted therapy. Color code for bottom right part: light green cells, angiogenic vascular cells; orange cells, tumor cells.

Considering the prominent significance of endothelial MPs (EMPs) in various pathophysiological events, the human umbilical vein endothelial cells (HUVECs) were selected as the model donor cells for EMP production. Initially, we confirmed that no cytotoxicity was detected during the membrane biotinylation of donor cells (Figure S1). By employing flow cytometry (Figure S2) and fluorescence microscopy observation (Figure S3), we then verified that membrane biotinylation and subsequent QD labeling could be conveniently realized on the donor cells by culturing them with DSPE-PEG-biotin for several days. To further obtain EMPs with biotinylated membrane, the as-prepared biotinylated HUVECs were starved in basic medium for EMP release (Figures S4 and S5).

To assess the specificity and efficiency of our proposed labeling strategy for MPs, the EMPs purified from CFSE-labeled HUVECs with or without membrane biotinylation were incubated with SA-QDs, and then observed under a fluorescence microscope or analyzed with flow cytometry following removal of the unbound QDs by sucrose gradient centrifugation (Figure S6). As shown in Figure 1 a, concurrent QD and CFSE fluorescence signals could be observed in biotinylated EMPs, but only CFSE and nearly no QD signal could be detected in the EMPs isolated from normal HUVECs. Also, the electron micrographs verified the specific binding of SA-QDs onto the surface membrane of biotinylated EMPs (Figure 1 b, red arrows). The results from flow cytometric analysis (Figure 1 c) further demonstrated that both the percentage of QD-labeled events and QD fluores-

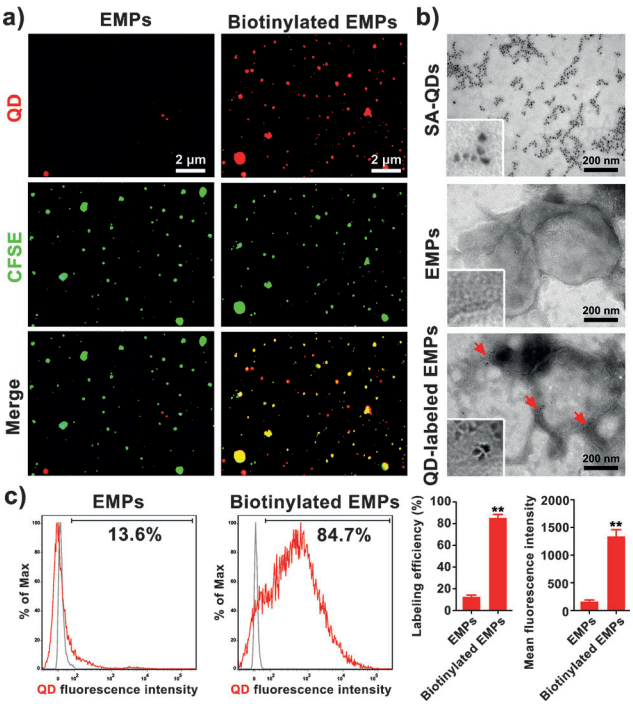


***Figure 1.*** Specificity and efficiency of the membrane biotinylation-based QD labeling strategy for MPs. a) Fluorescence images of EMPs or biotinylated EMPs after dual labeling with SA-QDs and CFSE. b) Transmission electron micrographs of EMPs or biotinylated EMPs after incubation with SA-QDs. c) Flow cytometry analysis of EMPs or biotinylated EMPs after labeling with SA-QDs. **, $P<0.01$ versus the normal EMP group.


© 2015 Wiley-VCH Verlag GmbH & Co. KGaA, Weinheim

cence intensity in biotinylated EMPs were markedly higher than those in the EMPs purified from normal HUVECs, thereby suggesting the good specificity of this labeling strategy. Besides valuable specificity, our membrane biotinylation-based QD labeling strategy also showed higher efficiency than the labeling strategy using indirect encapsulation of CFSE, PKH26, or QDs (Figure S7). All these results indicate that the membrane biotinylation-based labeling strategy has good specificity and high efficiency.

To determine whether the high specificity and efficiency of this membrane biotinylation-based labeling strategy were reproducible for MPs of different cellular origins, two other major types of cell-derived MPs, i.e., macrophage-derived MPs (MMPs) and tumor-derived MPs (TMPs), were then employed in this study. The results revealed that MMPs and TMPs, derived from biotinylated THP-1 cells and CAL-27 cells, respectively, were also successfully labeled with SA-QDs with good specificity and high efficiency (Figures S8 and S9). As shown in Table 1, the labeling efficiency and coefficient of variation (CV) for different types of MPs further prove that our proposed membrane biotinylation-based labeling strategy also has good universality and reliable reproducibility.

***Table 1:*** Membrane biotinylation-based QD labeling for MPs of different origins.

| Different types of MPs | Labeling efficiency [%] | Coefficient of variation [%] |
|---|---|---|
| EMPs | 85.3 | 3.8 |
| MMPs | 83.1 | 4.5 |
| TMPs | 86.3 | 5.4 |

As mentioned before, good biocompatibility is particularly important for the labeling of cell-derived MPs. To evaluate the influence of membrane biotinylation and QD labeling on MPs, the biotinylated EMPs were initially characterized by transmission electron microscopy (Figure S10), dynamic light scattering (Figure S11), and flow cytometry analysis (Figure S12). The results demonstrated that the biotinylated EMPs had a diameter of 100 nm to 1000 nm and highly expressed phosphatidylserine (PS) and the endothelial cell marker CD31, which is in line with the features of normal EMPs.[14] Moreover, the surface markers of EMPs were not affected by QD labeling, as evidenced by the concurrence of QDs with $PS^+/CD31^+$ expression (Figure S13). Meanwhile, real-time quantitative polymerase chain reaction (qPCR) and western blot analysis indicated that membrane biotinylation and QD labeling did not influence the mRNA or protein expression of characteristic molecules in EMPs (Figure S14). Then, uptake assays using endothelial progenitor cells (EPCs) as the recipient cells were performed to determine the cellular internalization of QD-labeled EMPs by considering CFSE-labeled EMPs as reference. As shown in Figure 2, both QD- and CFSE-labeled EMPs (white arrows) were effectively taken up by EPCs after short-term incubation, showing no significant difference in

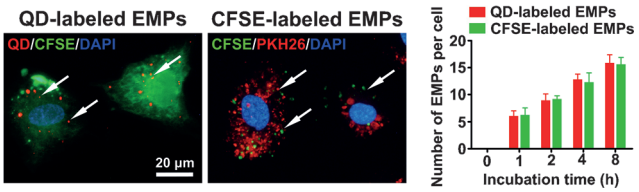


***Figure 2.*** Fluorescence imaging for cellular uptake of QD- or CFSE-labeled EMPs by EPCs after 2 h incubation (left). The number of labeled EMPs per cell was analyzed at different time points (right).

the uptake efficiency when observed statically at different time points. Thus, it can be concluded that the natural properties of EMPs, including the size, molecular composition, and capability to be internalized into target cells, are unaffected by membrane biotinylation or QD labeling, suggesting the excellent biocompatibility of this labeling strategy.

Collectively, the above results demonstrate that QD labeling of MPs is realized with a convenient procedure, good specificity, high efficiency, reliable reproducibility, and excellent biocompatibility through a donor-cell-assisted membrane biotinylation strategy. In addition to reliably conferring the highly valuable long-term traceability on MPs (Figure S15), this biofriendly labeling strategy, which utilizes the natural membrane phospholipid exchange of the donor cells, can meanwhile maximally preserve the natural properties and functions of MPs. Regarding the potential toxicity of the exposed QDs, we consider that surface labeling with an appropriate amount of carefully synthesized and modified QDs would not induce significant cytotoxicity to affect the laboratory research of MPs, which has been evidenced by our findings that the uptake of QD-labeled EMPs did not affect the viability of EPCs (Figure S16). Moreover, if necessary, the biotinylated MPs can be conveniently conjugated with more biocompatible QDs including our synthesized $Ag_2Se$ QDs.[15] Importantly, the biotinylated MPs can also be used as a versatile platform for efficient conjugation of biogenic MPs with a variety of functional nanomaterials according to different research demands by taking advantage of the high affinity between biotin and streptavidin, such as the magnetic nanospheres, which are powerful tools for rapid isolation and efficient detection.[16] This reliable and biofriendly labeling and functionalization strategy, which also shows particular compatibility with additional labeling techniques for the inner molecules of MPs, can provide high feasibility for future investigations and applications of MPs.

Here, in an attempt to investigate the in vivo implication of EMPs in human malignant melanoma, we injected nude mice bearing A2058 xenografts with QD-labeled EMPs. Firstly, the in vivo detectability of QD-labeled MPs was verified (Figure 3a). Figure 3b indicates that fluorescence signals for QD-labeled EMPs and QDs could be detected 24 h after intratumoral injection. The fluorescence signals of QDs alone were restrained to the injection point (white arrow), whereas the fluorescence signal of QD-labeled EMPs diffused toward the whole tumor site (red dashed cycle), thereby suggesting the potential tumor-targeting ability of EMPs.


© 2015 Wiley-VCH Verlag GmbH & Co. KGaA, Weinheim

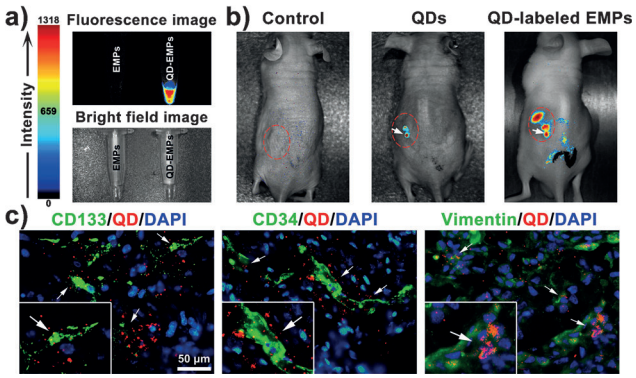


***Figure 3.*** In vivo imaging of QD-labeled EMPs. a) Fluorescence and bright field images of QD-labeled EMPs in the solvent. b) In vivo fluorescence photographs of A2058 human melanoma xenografts after injection with QD-labeled EMPs for 24 h. c) In situ visualization of QD-labeled EMPs on the frozen sections of A2058 xenografts.

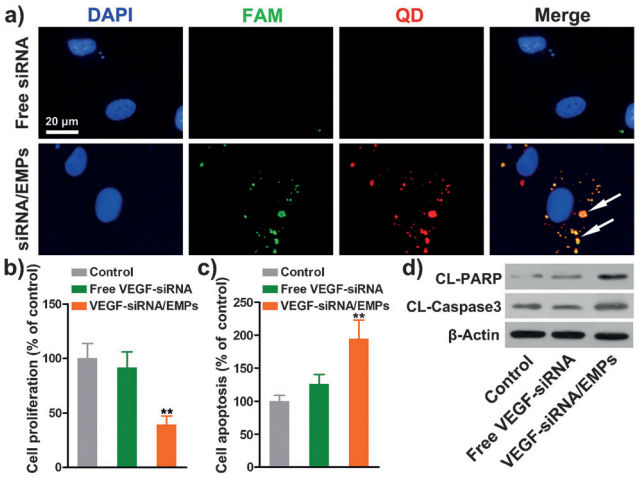


***Figure 4.*** EMP-mediated siRNA delivery in vitro. a) Fluorescence images of A2058 cells after incubation with free VEGF-siRNA or VEGF-siRNA loaded in QD-labeled EMPs (siRNA/EMPs). b) Proliferation of A2058 cells after indicated treatments. c) Apoptosis of A2058 cells after indicated treatments. d) The expression levels of apoptosis-related proteins in A2058 cells after indicated treatments. **, $P<0.01$ versus the control group.

Consistently, by contrast to the injection with QDs alone, much weaker fluorescence emission could be observed in the liver 24 h after intratumoral injection with QD-labeled EMPs (Figure S17). The in situ visualization assays on the frozen sections of A2058 xenografts also verified that positive QD signals (white arrows) could only be detected when injected with QD-labeled EMPs, mostly located in the cells positive for CD133 (EPC marker), CD34 (EC marker), and vimentin (tumor cell marker) expression (Figures 3c and S18), which was in line with our in vitro results (Figures 2 and S19).

Simultaneous targeting of multiple cellular components within the tumor microenvironment has been recently proven as one of the most potent strategies for tumor-targeted therapy.[17] In this regard, we proposed to produce traceable biogenic nanovectors for tumor-targeted delivery of therapeutic small interference RNA (siRNA) based on combined QD labeling and siRNA loading of EMPs. As indicated in Scheme 1, the purified biotinylated MPs were electroporated with carboxyfluorescein (FAM)-labeled siRNA ($siRNA^{FAM}$) against vascular endothelial growth factor (VEGF), a critical growth factor for both melanoma and angiogenic vascular cells.[18] The siRNA-loaded biotinylated MPs were then labeled with SA-QDs to form functionalized MPs. Such MPs are versatile for bioimaging at different levels, and can meanwhile deliver the therapeutic siRNA to induce tumor-targeted inhibition by taking virtue of their selective uptake by target cells, including tumor and angiogenic vascular cells.

As shown in Figure S20, our results demonstrated that $siRNA^{FAM}$ was efficiently loaded into EMPs in a concentration-dependent manner. The flow cytometry analysis (Figure S21) and fluorescence microscopy observation (Figure S22) further verified the high co-localization efficiency of $siRNA^{FAM}$ and QD-labeled EMPs. Moreover, the encapsulated $siRNA^{FAM}$ within QD-labeled EMPs exhibited no significant change over 48 h (Figure S23), which suggests the favorable stability of siRNA-loaded EMPs. Then, we confirmed that the VEGF-siRNA was efficiently delivered into A2058 cells and EPCs through cellular internalization of the siRNA-loaded EMPs, as demonstrated by the intracellular co-localization of FAM with QD signals (Figures 4a and S24, white arrows). The results further demonstrated that, after incubation with VEGF-siRNA-loaded EMPs but not free VEGF-siRNA, the mRNA expression and protein secretion levels of VEGF and several other related factors in A2058 cells (Figure S25) and EPCs (Figure S26) were significantly down-regulated, thereby suggesting favorable gene-silencing efficiency. Our results also showed that VEGF-siRNA-loaded EMPs exhibited proliferation inhibition (Figures 4b and S27) and apoptosis induction (Figures 4c and S28) effects on A2058 cells and EPCs, which correlated with the altered expression of apoptosis-related proteins (Figures 4d and S29).

After verification of the great potential of EMPs in therapeutic siRNA delivery in vitro, we then evaluated their in vivo efficiency. As shown in Figure 5a, intratumoral injection with VEGF-siRNA-loaded EMPs reduced the growth of A2058 xenografts when compared with the free VEGF-siRNA and control groups, and no obvious toxicity was observed (Figure S30). Consistently, the expression levels of cytoplasmic VEGF and nuclear Ki-67 were down-regulated

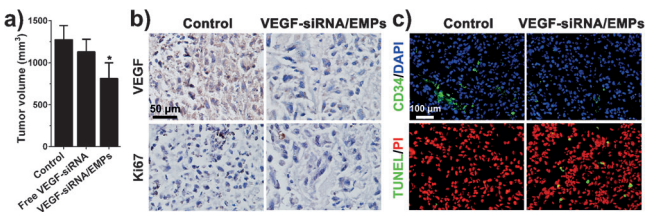


***Figure 5.*** VEGF-siRNA-loaded EMPs exhibited tumor-inhibitory effects in vivo. a) The volume of A2058 xenografts after treatment with vehicle control, free VEGF-siRNA or VEGF-siRNA-loaded EMPs. *, $P<0.05$ versus the control group. b) The expression of VEGF and proliferation marker Ki-67 in A2058 tumors evaluated by immunohistochemistry. c) The microvessels and apoptotic cells determined by CD34-immunofluorescence and in situ TUNEL assay.

 © 2015 Wiley-VCH Verlag GmbH & Co. KGaA, Weinheim 

in the tumor tissues injected with VEGF-siRNA-loaded EMPs (Figure 5b), correlating with the decrease in CD34-positive microvessels and increase in apoptotic cells (Figure 5c). All the above results suggested that biogenic EMPs could be applied as tumor-targeted vectors for therapeutic siRNA delivery by utilizing their inherent ability in cell targeting and biomolecule conveying.

In summary, our present study proposed the first biofriendly and reliable strategy for labeling and functionalizing cell-derived MPs, which exhibits a number of unprecedented advantages. Based on our proposed donor-cell-assisted membrane biotinylation strategy, QD-labeled MPs were obtained in a convenient procedure and with good specificity, high efficiency, reliable reproducibility, and excellent biocompatibility. This strategy not only conferred the highly valuable traceability on MPs, but also maximally preserved the natural properties and functions of MPs. In virtue of the excellent traceability and biocompatibility, we provided the first direct evidence that EMPs may greatly contribute to the progression of malignant melanoma through their dual uptake by tumor and angiogenic vascular cells. More importantly, by further integration of biofriendly QD labeling and efficient siRNA encapsulation, the biogenic MPs were successfully transformed from natural intercellular communicators to functionalized nanovectors for combined bioimaging and tumor-targeted therapy. This study may potentially revolutionize the field with regard to the investigation and application of cell-derived MPs, and meanwhile open new avenues for generating multifunctional nanovectors.

Received: October 18, 2014
Published online: November 24, 2014

**Keywords:** biogenic vesicles · cell-derived microparticles · nanoparticles · quantum dots · targeted delivery

[1] S. F. Mause, C. Weber, *Circ. Res.* **2010**, *107*, 1047 – 1057.
[2] F. Raposo, W. Stoorvogel, *J. Cell. Biol.* **2013**, *200*, 373 – 383.
[3] X. Loyer, A. C. Vion, A. Tedgui, C. M. Boulanger, *Circ. Res.* **2014**, *114*, 345 – 353.
[4] K. Tang, Y. Zhang, H. Zhang, P. Xu, J. Liu, J. Ma, M. Lv, D. Li, F. Katirai, G. X. Shen, G. Zhang, Z. H. Feng, D. Ye, B. Huang, *Nat. Commun.* **2012**, *3*, 1282.
[5] Y. Zhang, L. Li, J. Yu, D. Zhu, Y. Zhang, X. Li, H. Gu, C. Y. Zhang, K. Zen, *Biomaterials* **2014**, *35*, 4390 – 4400.
[6] A. K. Silva, J. Kolosnjaj-Tabi, S. Bonneau, I. Marangon, N. Boggetto, K. Aubertin, O. Clément, M. F. Bureau, N. Luciani, F. Gazeau, C. Wilhelm, *ACS Nano* **2013**, *7*, 4954 – 4966.
[7] K. Andriola Silva, R. Di-Corato, T. Pellegrino, S. Chat, G. Pugliese, N. Luciani, F. Gazeau, C. Wilhelm, *Nanoscale* **2013**, *5*, 11374.
[8] H. C. van der Heyde, I. Gramaglia, V. Combes, T. C. George, G. E. Grau in *Flow Cytometry Protocols*, *Vol. 699* (Eds.: T. S. Hawley, R. G. Hawley), Springer, Heidelberg, **2011**, pp. 337 – 354.
[9] U. Resch-Genger, M. Grabolle, S. Cavaliere-Jaricot, R. Nitschke, T. Nann, *Nat. Methods* **2008**, *5*, 763 – 775.
[10] S. Montoro-García, E. Shantsila, F. Marín, A. Blann, G. Y. Lip, *Basic Res. Cardiol.* **2011**, *106*, 911 – 923.
[11] S. L. Liu, Z. L. Zhang, Z. Q. Tian, H. S. Zhao, H. B. Liu, E. Z. Sun, G. F. Xiao, W. Zhang, H. Z. Wang, D. W. Pang, *ACS Nano* **2012**, *6*, 141 – 150.
[12] L. Wen, Y. Lin, Z. H. Zheng, Z. L. Zhang, L. J. Zhang, L. Y. Wang, H. Z. Wang, D. W. Pang, *Biomaterials* **2014**, *35*, 2295 – 2301.
[13] B. H. Huang, Y. Lin, Z. L. Zhang, F. Zhuan, A. A. Liu, M. Xie, Z. Q. Tian, Z. Zhang, H. Wang, D. W. Pang, *ACS Chem. Biol.* **2012**, *7*, 683 – 688.
[14] F. Jansen, X. Yang, M. Hoelscher, A. Cattelan, T. Schmitz, S. Proebsting, D. Wenzel, S. Vosen, B. S. Franklin, B. K. Fleischmann, G. Nickenig, N. Werner, *Circulation* **2013**, *128*, 2026 – 2038.
[15] Y. P. Gu, R. Cui, Z. L. Zhang, Z. X. Xie, D. W. Pang, *J. Am. Chem. Soc.* **2012**, *134*, 79 – 82.
[16] C. Y. Wen, L. L. Wu, Z. L. Zhang, Y. L. Liu, S. Z. Wei, J. Hu, M. Tang, E. Z. Sun, Y. Gong, J. Yu, D. W. Pang, *ACS Nano* **2014**, *8*, 941 – 949.
[17] N. E. Sounni, A. Noel, *Clin. Chem.* **2013**, *59*, 85 – 93.
[18] V. Trapp, B. Parmakhtiar, V. Papazian, L. Willmott, J. P. Fruehauf, *Angiogenesis* **2010**, *14*, 305 – 315.

 © 2015 Wiley-VCH Verlag GmbH & Co. KGaA, Weinheim 